

See discussions, stats, and author profiles for this publication at: <https://www.researchgate.net/publication/261214582>

Multicomponent Diffusion and Reaction in Three-Dimensional Networks: General Kinetics

ARTICLE *in* JOURNAL OF INDUSTRIAL AND ENGINEERING CHEMISTRY · MAY 1997

Impact Factor: 3.51

CITATIONS

25

READS

29

2 AUTHORS, INCLUDING:



Frerich J Keil

Technische Universität Hamburg-Harburg

205 PUBLICATIONS 4,825 CITATIONS

SEE PROFILE

Multicomponent Diffusion and Reaction in Three-Dimensional Networks: General Kinetics[†]

Christina Rieckmann and Frerich J. Keil*

Department of Chemical Engineering, Technical University of Hamburg-Harburg, Eissendorfer Strasse 38, D-21073 Hamburg, Germany

Over the last 10 years the design of catalyst particles and porous structures has made considerable progress. Due to the complicated interaction of diffusion and reaction in catalysts, more detailed models of porous structures are needed. We have based our model on a three-dimensional network of interconnected cylindrical pores as pore model, although the treatment is applicable to alternative pore geometries, e.g., slit pores. The network assumed has predefined distributions of pore radii, connectivity, and porosity. Mass transport in the individual pores of the network is described by the dusty-gas model. In contrast to previous publications, the present network model can be applied to any common reaction kinetics. This becomes quite inevitable in order to make three-dimensional network models applicable to practical problems in industry. To solve the mass balances within the entire network, the mass balances for individual pores have to be solved simultaneously, since these mass balances are coupled by the boundary conditions at the nodes of the network. The system of differential equations has been solved by the finite-difference method. To solve the resulting large nonlinear system, a Schur complement method was employed. Due to a decoupling technique, the Schur complement method has relatively small computer storage requirements. The use of the algorithm is demonstrated for a complex reaction network.

Introduction

Porous catalyst supports are in widespread use in the chemical industry. Reactants diffuse into the void space of the support and react, and products formed diffuse out of the pellet. Multicomponent diffusion within the catalyst supports, which have a very complicated geometrical structure, has to be described. Molecular, Knudsen, and surface diffusion can all occur. On fractal surfaces anomalous diffusion will take place, and in microporous materials, configurational diffusion may be the dominating mass transport mechanism. A quite useful approximation based on Boltzmann's equation, the dusty-gas model, has been developed (Mason and Malinauskas (1983)). This model describes the molecular diffusion, Knudsen diffusion, viscous flux, and, in principle, the surface diffusion, with sufficient accuracy.

However, the dusty-gas model avoids any assumption about the internal structure of the solid. Although the dusty-gas model can be adapted to any pellet geometry, empirical factors such as pore voidage and tortuosity are mostly employed.

The fundamentals underlying surface, configurational, and anomalous diffusion are still under investigation. Molecular dynamics and Monte Carlo approaches are the preferred methods of calculation for these transport mechanisms. Following the attempts of Wakao and Smith (1962), Johnson and Stewart (1965), and Foster and Butt (1966) to describe the porous structure of catalyst pellets, capillary Bethe lattices and random networks were employed to model the structure of porous materials. Reyes and Jensen (1985), Beeckman et al. (1978), and Beeckman and Froment (1980) have also used a Bethe lattice repre-

sentation of the porous medium. In this model no closed loops and a fixed connectivity are employed. Gavalas and Kim (1981) and Petropoulos et al. (1991) have introduced capillary networks, whereas Sharratt and Mann (1987) have studied the properties of random networks.

This type of model describes the voidage as interconnected pores with a random distribution of pore sizes (e.g., pore radii for cylindrical pores). The pore size distribution can be obtained experimentally, from either nitrogen sorption measurements or mercury porosimetry. These measurements can be evaluated by a variety of methods (Dullien (1992)). Other approaches are statistical-mechanical techniques (Seaton et al. (1989)) or reconstruction calculations derived from Wicke-Kallenbach measurements (Keil and Schreiber (1994)). The mean coordination number (connectivity) can be obtained experimentally (Seaton (1991); Liu et al. (1992); Portsmouth and Gladden (1991); Scharfenberg et al. (1996)). As has been found by Hollewand and Gladden (1992a,b), one should differentiate between distinct but interconnected micro- and macroporous networks of pores, to provide a realistic representation of a bimodal porous network. These networks are advantageous in several respects:

- (1) The effect of connectivity of the pore space is taken into account.
- (2) Any type of network can be employed.
- (3) Any pore size distribution and any pore geometry, e.g., cylindrical or slitlike pore, can be used.
- (4) It is possible to model local heterogeneities, e.g., spatial variation in mean pore size.
- (5) Any distribution of catalytic active centers may be taken into account.
- (6) Percolation phenomena can be described.

Recent applications of network models are presented by Arbabi and Sahimi (1991a,b), Sahimi (1992), McGreavy et al. (1992), and Zhang and Seaton (1994) among others. Keil and Rieckmann (1994) have opti-

* Author to whom correspondence is addressed. Telephone: +49 40 7718 3042. Fax: +49 40 7718 2145. E-mail: keil@tu-harburg.d400.de.

[†] This paper is dedicated to Prof. Gilbert Froment on the occasion of his 65th birthday.

mized catalyst pore structures for the hydrodemetalation process with the aid of three-dimensional lattice models.

One has to bear in mind that in lattice-based models diffusion and reaction phenomena are limited to the lattice framework. In order to remove this limitation, Drewry and Seaton (1995), among others, have modeled porous catalysts as randomly sized and located spheres representing the support and active sites.

During the last 10 years, the concept of fractality has been used increasingly in heterogeneous catalysis. For reviews of this approach Avnir (1989), Bunde and Havlin (1994), Sahimi (1995), or Keil (1996) may be consulted.

In the present work the authors have modeled multicomponent diffusion and reaction in networks of pores. In the past several authors have published papers concerning diffusion and reactions with first-order kinetics in networks. In order to make three-dimensional networks applicable to practical problems in the chemical process industry, they have to be suitable for any type of common chemical kinetic equations. The basic features of the present paper are as follows:

(1) Multicomponent diffusion has been modeled using a Maxwell-Stefan approach.

(2) Multicomponent diffusion and reaction occur in a random network of interconnected pores with a pre-defined average connectivity and distribution of pore radii, whereby any type of network can be employed.

(3) Pores with smooth or fractal walls and of any shape may be used as long as transport behavior within the pores is known.

(4) Percolation phenomena can be studied.

(5) Different distributions of active centers may be investigated.

(6) In contrast to previous work, any common type of reaction kinetics may be applied. This is the most important aspect of the present work. In the present paper only the isothermal case was considered. Recently developed numerical techniques have led to a considerable reduction of computer memory requirements for such calculations. The algorithm will be applied to a reaction mechanism suggested by Beyne and Froment (1993), who applied it to the ZSM-5 network, using percolation theory.

Model

The catalytic active crystallites are distributed within the pore space of a support. The reactants have to diffuse into the pore space, where they react at the active centers to form products. The types of diffusion (Knudsen diffusion, bulk or molecular diffusion, configurational diffusion, surface diffusion, anomalous diffusion) depend on the size of the pores, the molecules involved, the operating conditions, and the surface geometry of the pores. A realistic model of pore space is especially important to describe plugging phenomena as the percolation threshold is approached. The authors have taken a three-dimensional random cubic network of interconnected cylindrical pores. The pore walls were assumed to be smooth, but an extension to fractal walls is straightforward. Other networks, e.g., Voronoi grids, and other pore geometries could have been taken just as well. An average connectivity of the pores of up to 6 can be selected. If necessary, a larger number, as has been modeled by Keil and Rieckmann (1994), can be introduced, but most supports in use exhibit connectivities between 3 and 6. Jerauld et al. (1984) and

Winterfeld et al. (1981) have shown that, as long as the average coordination number of a topologically-disordered system is equal to the coordination number of a regular network, the transport properties of the two systems are essentially identical. The pore radii are randomly distributed over the network so as to meet a predetermined overall distribution function. This function may be obtained from BET measurements or mercury porosimetry. Catalyst pellets often have a bimodal pore size distribution. As a consequence of the preparation process, they consist of microporous particles with interstitial macropores. The network of macropores extends throughout the entire pellet. The macropores are responsible for transport. We have thus used a microporous network augmented with a network of interconnected macropores.

As the pore network is composed of single cylindrical pores of different diameters, the dusty-gas model for a single pore was used as a starting point. The dusty-gas model combines the contributions of Knudsen and molecular fluxes

$$\frac{dc_i}{dw} = \sum_{\substack{j=1 \\ j \neq i}}^{N_K} \frac{J_j^D x_i - J_i^D x_j}{D_{ij}(p)} - \frac{J_i^D}{D_{ii}^K(r_p, p)} \quad (1)$$

as well as the viscous flux

$$\mathbf{J}^V = -\mathbf{c} \frac{r_p^2}{8\eta} \frac{dp}{dw} = -\mathbf{c} ZRT \frac{r_p^2}{8\eta} \frac{dc_{tot}}{dw} \quad (2)$$

with

$$c_{tot} = \sum_{i=1}^{N_K} c_i \quad (3)$$

The explicit equation for the diffusive fluxes takes the form of a matrix equation:

$$\mathbf{J}^D = -\mathbf{D}^{-1}(r_p, \mathbf{c}, p) \frac{d\mathbf{c}}{dw} \quad (4)$$

with

$$D_{ij}(r_p, \mathbf{c}, p) = \begin{cases} -\frac{x_i}{D_{ij}(p)} & \forall i \neq j \\ \frac{1}{D_{ii}^K(r_p, p)} + \sum_{\substack{h=1 \\ h \neq i}}^{N_K} \frac{x_h}{D_{ih}(p)} & \forall i = j \end{cases} \quad (5)$$

Diffusive and viscous fluxes are summed to yield the total molar flow:

$$\mathbf{J} = \mathbf{J}^D + \mathbf{J}^V \quad (6)$$

If necessary, a term for the surface diffusion may be added. This is important for reactions at elevated pressure.

Chemical reactions occur within the pores. The material balance for the components within a single cylindrical pore under isothermal conditions is given by

$$\frac{d\mathbf{J}}{dw} - \frac{2}{r_p} \nu \mathbf{r}(\mathbf{c}, T) = \mathbf{0} \quad (7)$$

which thus gives

$$-RT \frac{r_p^2}{8\eta} \left(\mathbf{c} \frac{d^2 c_{tot}}{dw^2} + \frac{dc}{dw} \frac{dc_{tot}}{dw} \right) - \mathbf{D}^{-1} \frac{d^2 \mathbf{c}}{dw^2} - \frac{d}{dw} (\mathbf{D}^{-1}) \frac{dc}{dw} - \frac{2}{r_p} \nu \mathbf{r}(\mathbf{c}, T) = \mathbf{0} \quad (8)$$

In a pore network, the single pores are connected at the nodes of the network. No adsorption or chemical reaction is assumed to take place at the nodes. The fluxes of the species that enter a node must therefore be equal to the fluxes leaving the node. At the inner nodes of the network, an equation similar to Kirchhoff's law holds:

$$\sum_{ip} \mathbf{J}_{ip} r_{p,ip}^2 = \mathbf{0} \quad (9)$$

At the outer surface nodes of the network a boundary layer is assumed. The flux from the bulk phase into a single pore is

$$\mathbf{J} = \beta(\mathbf{c}_b - \mathbf{c}_s) \quad (10)$$

For each component a different value of β may be chosen. Multicomponent effects in the external mass transfer could have been included (Taylor and Krishna (1993)).

The set of equations that has to be solved in the network is

(a) for each pore of the network equation (7):

$$\frac{d\mathbf{J}(\mathbf{c}|_{i,j,k,ip})}{dw} - \frac{2}{r_p|_{i,j,k,ip}} \nu \mathbf{r}(\mathbf{c}|_{i,j,k,ip}, T) = \mathbf{0} \quad \forall i, j, k \in [1, N] \quad \forall ip \in [1, 3] \quad (11)$$

(b) for each inner node of the network equation (9):

$$\mathbf{J}'(\mathbf{c}|_{i-1,j,k,1}) + \mathbf{J}'(\mathbf{c}|_{i,j-1,k,2}) + \mathbf{J}'(\mathbf{c}|_{i,j,k-1,3}) + \sum_{ip=1}^3 \mathbf{J}'(\mathbf{c}|_{i,j,k,ip}) = \mathbf{0} \quad i, j, k \in [2, N-1] \quad (12)$$

with

$$\mathbf{J}' = \mathbf{J} \pi r_p^2$$

(c) for each outer node of the network equation (10):

$$\mathbf{J}(\mathbf{c}|_{i,j,k}) = \beta(\mathbf{c}_b - \mathbf{c}_{s,i,j,k}) \quad \forall i, j, k = 1 \quad \forall i, j, k = N \quad (13)$$

Isolated pore clusters are removed from the network by a Hoshen-Kopelman algorithm (1976) as these clusters do not contribute to the species' fluxes within the network.

Micro-Macro-Scaling. The outer dimension of the network has to be equal to that of the actual pellet in order to cover the whole Thiele modulus range.

The porosity of the network is the ratio of the pore volume to the outer volume of the network cube. Although networks with several thousand nodes were employed, the total porosity in a pore network is orders of magnitude less than that of a real catalyst. The same is true for the volume ratio of micro- to macropores in a pore and for the molar fluxes into and out of the nodes. The micro- and macropore fluxes have therefore been scaled in the following manner:

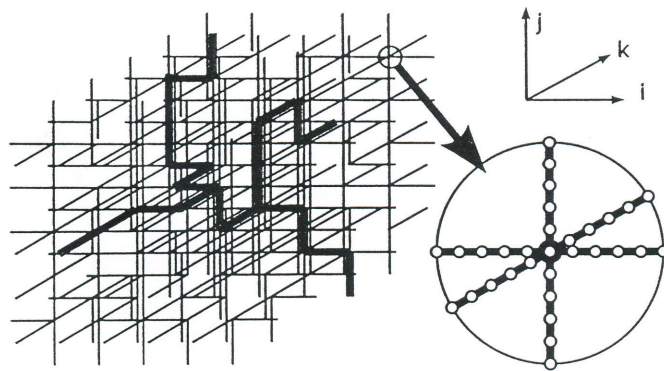


Figure 1. Discretization of the pore network.

$$\mathbf{J}_M = \mathbf{J}_{M,net} \frac{V_{M,cat}}{V_{M,net}} \quad (14)$$

$$\mathbf{J}_m = \mathbf{J}_{m,net} \frac{V_{m,cat}}{V_{m,net}} \quad (15)$$

This scaling implies a locally homogeneous pellet structure. If these corrections are omitted, unrealistic results will be obtained from pore structure optimization (Keil and Rieckmann (1994)).

Solution of the Model Equations

For each individual pore one has to solve a boundary value problem. The boundary conditions of different pores are coupled by Kirchhoff's law. The boundary value problems of the pores have to be solved simultaneously. The model equations were solved by the finite-difference method.

Each pore was discretized in the axial direction (see Figure 1). Derivatives were approximated by finite-difference formulas. At interior points of the pores, the following central difference formulas were used:

$$\frac{dc}{dw} = \frac{c_{k+1} - c_{k-1}}{2\Delta w} + O(\Delta w^2) \quad (16)$$

$$\frac{d^2 c}{dw^2} = \frac{c_{k+1} - 2c_k + c_{k-1}}{\Delta w^2} + O(\Delta w^2) \quad (17)$$

At the pore ends, one-sided difference formulas were employed:

$$\frac{dc}{dw} \Big|_{w=0} = \frac{-3c_0 + 4c_1 - c_2}{2\Delta w} + O(\Delta w^2) \quad (18)$$

$$\frac{dc}{dw} \Big|_{w=L_p} = \frac{c_{n-2} - 4c_{n-1} + 3c_n}{2\Delta w} + O(\Delta w^2) \quad (19)$$

Introducing these difference formulas into eqs 11–13 leads to a large system of nonlinear equations:

$$\mathbf{F}(\mathbf{c}) = \mathbf{0} \quad (20)$$

The structure of the Jacobian matrix is shown in Figure 2. The equations for the pores are located in the upper part of the matrix and those for the nodes in the lower part. The entries for the concentrations within the pores are to be found on the left-hand side and the concentrations at the nodes on the right-hand side.

Due to the central difference formulas, the material balances inside the single pores lead to a tridiagonal

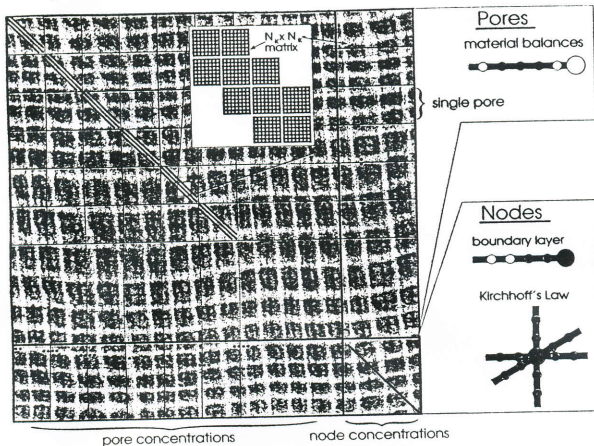


Figure 2. Structure of the Jacobian matrix.

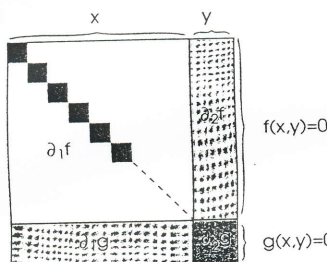


Figure 3. Macrostructure of the Jacobian matrix.

band of $N_k \times N_k$ matrices. At the ends of each pore the equations are coupled with the concentrations at the nodes.

The equations for the nodes lead to a diagonal band of $N_k \times N_k$ matrices. For each of the pores entering a node there are two entries in the form of $N_k \times N_k$ matrices, because of the one-sided difference formulas at the pore ends.

The matrix is nonsymmetric and not diagonally dominant. This makes the solution of the present nonlinear system of equations difficult. The eigenvalues of the matrix range from -1.9×10^5 to $+1.8 \times 10^{-2}$.

Schur Complement Method. The large system of nonlinear equations was solved by a Schur complement method. It is a Gauss-Seidel Newton-type iteration for solving nonlinear systems with a block sparsity pattern of the Jacobian. Such methods have been discussed under the designation of Newton-type decomposition by Hoyer and Schmidt (1984) and Schmidt et al. (1985).

The structure of the Jacobian matrix will first be discussed briefly. Obviously the matrix consists of two parts, the nonlinear system of the pores and the nonlinear system of the nodes, which are coupled with one another. This is illustrated in Figure 3, which presents the macrostructure of Figure 2. The large black matrix block $\partial_1 f$, which is actually much larger than shown in this figure, is coupled with the smaller dark-gray matrix block $\partial_2 g$ by the two light-gray matrix blocks $\partial_2 f$ and $\partial_1 g$. As will be described in detail below, the solution strategy is to separate the two systems and solve them iteratively. The advantage of this method is that the system of the pores will be split up into independent subsystems. The material balances of each single pore (the black matrix blocks in Figure 3) can be solved independently from the other ones. As the whole Jacobian matrix need not be stored, the computer storage requirements are reduced considerably. This is the primary advantage of the Schur complement approach.

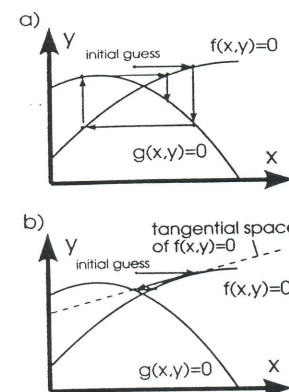


Figure 4. Iterative solution methods for two coupled nonlinear subsystems: (a) fixpoint iteration; (b) Newton method (Schur complement method).

To demonstrate the method, we introduce the following notation (see also Figure 3):

\mathbf{x} = vector of the concentrations within the pore,

\mathbf{y} = vector of the concentrations at the nodes,

$\mathbf{f}(\mathbf{x},\mathbf{y})$ = system of nonlinear equations for the pores, and

$\mathbf{g}(\mathbf{x},\mathbf{y})$: system of nonlinear equations for the nodes, with the Jacobian matrix as follows:

$$\begin{pmatrix} \partial_1 \mathbf{f} & \partial_2 \mathbf{f} \\ \partial_1 \mathbf{g} & \partial_2 \mathbf{g} \end{pmatrix}$$

We will illustrate the solution method in Figure 4 for the two-dimensional case; that is to say, \mathbf{x} and \mathbf{y} are of dimension one.

The simplest approach to solve the equations iteratively is a fixpoint iteration (see Figure 4a): After an initial guess of \mathbf{x}^0 and \mathbf{y}^0 , $\mathbf{f}(\mathbf{x},\mathbf{y})$ can be solved as a function of \mathbf{x} , keeping \mathbf{y} constant. Then $\mathbf{g}(\mathbf{x},\mathbf{y})$ is solved as a function of \mathbf{y} , keeping \mathbf{x} constant. This procedure is repeated until convergence is achieved. Obviously, this method can only converge linearly, and in half of the cases it would actually diverge, for example, if the inverse solution path in Figure 4a were to be followed.

Another approach to solving the equations iteratively is a Newton-type method (see Figure 4b). As with fixpoint iteration, after an initial guess of \mathbf{x}^0 and \mathbf{y}^0 , $\mathbf{f}(\mathbf{x},\mathbf{y})$ is solved as a function of \mathbf{x} , keeping \mathbf{y} constant. A Newton step is then carried out. The function $\mathbf{g}(\mathbf{x},\mathbf{y})$ is solved in the tangential space of $\mathbf{f}(\mathbf{x},\mathbf{y})$. This procedure is repeated until convergence is achieved. This method may also diverge. Like all Newton methods it has a convergence radius, but with a quite good initial guess, it converges quadratically. In Table 1 the algorithm of the Schur complement method is presented. To obtain global convergence a homotopy algorithm was employed.

The nonlinear systems for the single pores in step 1 in Table 1 were solved by a damped Newton method. We have used the code NLEQ1S from the library "codelib" of the Konrad-Zuse-Zentrum für Informationstechnik Berlin. Details of the algorithms and applications are given by Deuflhard (1997) and Nowak and Weimann (1990). The linear solver used in this code is the well-known MA28-package developed by Duff (1977, 1982), which employs a direct sparse mode elimination technique.

The Jacobian matrix of the Newton step 2 in Table 1 is the Schur complement of $\partial_1 \mathbf{f}$. The structure of the Schur complement is presented in Figure 5. It clearly shows the structure of a cubic network with a con-

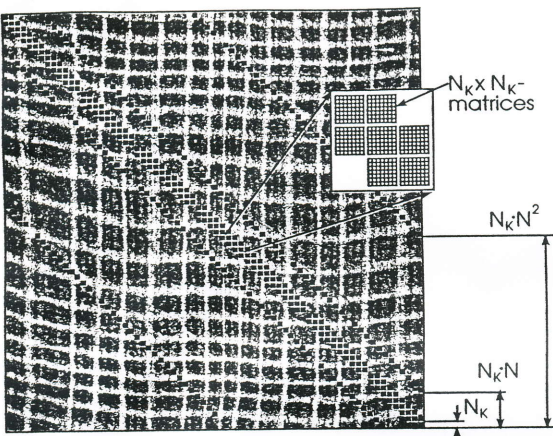
Figure 5. Structure of the Schur complement of $\partial_1 f$.

Table 1. Algorithm of the Schur Complement Method

- (0) an initial guess for the concentrations x^0, y^0
- (1) an approximate solution of the nonlinear systems of the single pores by means of a damped Newton method

$$x^{v+1/2} = x^v - \partial_1 f^{-1} \cdot f(x^v, y^v)$$
- (2) a Newton step in the tangential space
 - the calculation of the Jacobian matrix in the tangential space (Schur complement of $\partial_1 f$)

$$\partial G^v = (\partial_2 g - \partial_1 g \cdot \partial_1 f^{-1} \cdot \partial_2 f)(x^{v+1/2}, y^v)$$
 - the solution of the linear system

$$\partial G^v \cdot d_v = -g(x^{v+1/2}, y^v)$$
 - the calculation of the new iterate of the concentration vector

$$\begin{bmatrix} x^{v+1} \\ y^{v+1} \end{bmatrix} = \begin{bmatrix} x^{v+1/2} \\ y^{v+1} \end{bmatrix} + \begin{bmatrix} -\partial_1 f^{-1} \cdot \partial_2 f(x^{v+1/2}, y^v) \\ I \end{bmatrix} \cdot d_v$$
- (3) return to (1) until convergence is achieved

nectivity of less than 6. Next to the main block diagonal there are block diagonals at a distance of N_K , of NN_K and of N^2N_K , where N is the number of nodes for each of the three dimensions of the network and N_K is the number of components. Missing blocks in the block diagonals signify that the corresponding pores do not exist. For example, a missing block in the second upper block diagonal means that there is no pore in the y -direction at the node which corresponds to this matrix row.

Example

The algorithm can be adapted to any common form of reaction kinetics, which makes it employable to industrial problems. Using the algorithm described in the previous paragraphs, one has to provide the following experimental data: (1) rate expressions of the intrinsic kinetics; (2) distribution of pore radii and void fractions, taken from BET or mercury porosity measurements; (3) connectivity found by the method presented by, e.g., Seaton (1991) from BET measurements; (4) binary transport parameters (may also be calculated if not available).

As an example, the authors have used the reaction kinetics of a coking reaction of a reaction scheme described by Beyne and Froment (1993), suitable for modeling the deactivation of a ZSM-5 catalyst due to

Table 2. Reaction Scheme and Adsorption and Reaction Rate Constants

step	constant
(i) $A + l \rightleftharpoons A_l$	K_A
(ii) $A_l \rightarrow B_l$	k_{AB}
(iii) $B_l \rightarrow B + l$	K_B
(iv) $A_l \rightarrow C_p$	k_{iB}
(vi) $C_p + A \rightarrow C_g$	k_{gA}
(vii) $C_p + B \rightarrow C_g$	k_{gB}
(viii) $C_g + A \rightarrow C_g$	k_{gA}
(ix) $C_g + B \rightarrow C_g$	k_{gB}
(x) $C_g + A \rightarrow C_t$	k_{tA}
(xi) $C_g + B \rightarrow C_t$	k_{tB}

Table 3. Data Used for the Simulations

r_m	2×10^{-8}	m
r_M	1.5×10^{-7}	m
ϵ_m	0.124	
ϵ_M	0.05	
σ_m	0.2	
σ_M	0.2	
d_p	5×10^{-3}	m
$D_A = D_B$	10^{-5}	m^2/s
Z	4	
β	1	m/s
$K_A = K_B$	0.49	m^3/mol
$MW_A = MW_B$	86	g/mol
ρ_C	1800	kg/m^3
C_t	10^{-6}	mol/m^2
k_{AB}	0.175	1/s
$k_{iA} = k_{iB}$	10^{-4}	1/s
$k_{gA} = k_{gB}$	7.3×10^{-6}	$m^3/(mol s)$
$k_{tA} = k_{tB}$	7.3×10^{-6}	$m^3/(mol s)$
T	800	K

coke formation. The coke formation starts with the deposition of a coke precursor, proceeds through growth reactions, and stops under the influence of termination reactions. Both parallel and consecutive coking mechanisms were considered. The kinetic equations are of the Hougen-Watson type.

Three stages in the coke formation process were distinguished: (1) formation of coke precursor, C_p , from one or more reaction components; (2) coke growth: conversion of coke precursor into a growing species, C_g ; (3) termination of the coke growth: formation of a nonreactive coke, C_t .

The detailed mechanism of these three steps is shown in Table 2. The following reaction rate expressions correspond to the reaction steps of Table 2:

$$(ii) \quad r_{AB} = \frac{k_{AB} K_A C_t C_A}{1 + K_A C_A + K_B C_B} \left(1 - \frac{C_{Cl,acc}}{C_t}\right) \quad (21)$$

$$(iv) \quad r_{iA} = \frac{k_{iA} K_A C_t C_A}{1 + K_A C_A + K_B C_B} \left(1 - \frac{C_{Cl,acc}}{C_t}\right) \quad (22)$$

$$(v) \quad r_{iB} = \frac{k_{iB} K_B C_t C_B}{1 + K_A C_A + K_B C_B} \left(1 - \frac{C_{Cl,acc}}{C_t}\right) \quad (23)$$

$$(vi) \quad r_{pgA} = k_{gA} C_{Cp,acc} C_A \quad (24)$$

$$(vii) \quad r_{pgB} = k_{gB} C_{Cp,acc} C_B \quad (25)$$

$$(viii) \quad r_{gA} = k_{gA} C_{Cg,acc} C_A \quad (26)$$

$$(ix) \quad r_{gB} = k_{gB} C_{Cg,acc} C_B \quad (27)$$

$$(x) \quad r_{tA} = k_{tA} C_{Cg,acc} C_A \quad (28)$$

$$(xi) \quad r_{tB} = k_{tB} C_{Cg,acc} C_B \quad (29)$$

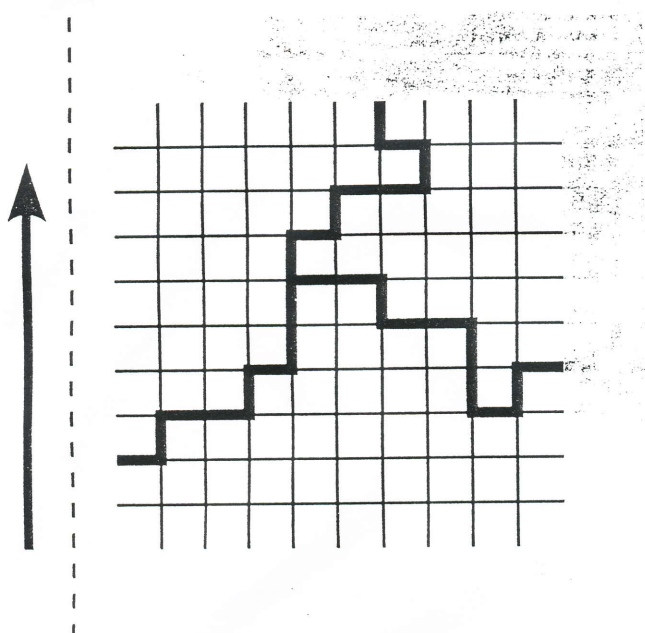


Figure 6. Boundary conditions at the network surfaces, two-dimensional section.

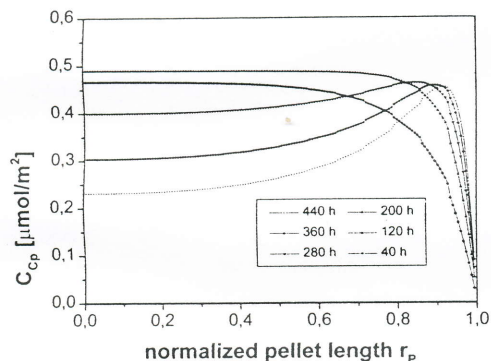


Figure 7. Concentration profiles of the active centers covered with the coke precursor Cp for consecutive coking. Parameter: time.

The catalyst data and the kinetic parameters listed in Table 3 have been used for the simulations. A microporous network augmented with a macroporous network was used. The micro- and macropore radii had a Gaussian distribution function with predetermined mean values r_m and r_M and predetermined standard deviations σ_m and σ_M .

Different boundary conditions were assumed for the outer surfaces of the network. One surface was assumed to be in contact with the bulk phase, and the other five surfaces were assumed to be closed with symmetry conditions pertaining (see a two-dimensional section in Figure 6).

The reaction mechanism consists of parallel coking reaction steps in which coke is formed from component A and consecutive coking reactions steps where coke is formed from component B. The concentrations and coke deposition profiles were calculated for the case of consecutive coking. A network of $10 \times 10 \times 10$ nodes has been used for the calculations. The network was generated separately five times in order to improve the averaging. The concentrations of the chemical species and the coke content have been averaged over all discretization points within the network that are at the same distance from the network surface. The concentration profiles of the active centers, C_{Cp} , covered with the coke precursor, Cp, are depicted in Figure 7. The profiles are given for different times.

In the case of consecutive coking the maximum of the coke precursor occurs initially at the center of the network, where the concentration of the coke-forming component B is at a maximum. With increasing time, the maximum migrates toward the surface of the network.

Conclusions

An efficient algorithm to calculate multicomponent concentration profiles for general kinetics within three-dimensional pore networks has been developed. The algorithm may be employed for any type of three-dimensional network and any pore shape. The pore walls may be smooth or of a fractal nature. Percolation processes can also be described by including a cluster counting algorithm. The present algorithm has been applied successfully to a complex example. It can be employed as a basic model for pore structure optimizations.

Acknowledgment

The authors are grateful to the BMBF for financial support (Grant No. 03D0015A) and the Fonds der Chemischen Industrie. They are also grateful to Prof. W. Mackens (TU Hamburg) and Prof. D. Agar (University of Dortmund) for valuable discussions.

Notation

- \mathbf{c} = vector of the concentrations, mol/m^3
 - \mathbf{c}_s = vector of the surface concentrations, mol/m^3
 - c_{tot} = total concentration, mol/m^3
 - C_A, C_B = concentration, mol/m^3
 - $C_t, C_{Cp}, C_{Cg}, C_{Ct}$ = surface concentration, mol/m^2
 - C_C = local coke concentration on the inner surface, kg/m^2
 - d_p = pellet diameter, m
 - D_{ij} = molecular diffusion coefficient, m^2/s
 - D_{ii}^K = Knudsen diffusion coefficient, m^2/s
 - \mathbf{D} = matrix of the diffusion coefficients, m^2/s
 - \mathbf{F} = vector of the deviation functions
 - = at the discretization points (eq 16), $\text{mol}/(\text{m}^3 \text{ s})$
 - = at the pore points (eq 7), $\text{mol}/(\text{m}^2 \text{ s})$, at the nodes (eqs 8 + 9)
 - \mathbf{J} = vector of the mole fluxes, $\text{mol}/(\text{m}^2 \text{ s})$
 - \mathbf{J}' = vector of the mole flows, mol/s
 - K = adsorption equilibrium constant, m^3/mol
 - k = reaction rate constant
 - L_p = pore length, m
 - N = number of nodes in each of the three dimensions of the network
 - N_K = number of components
 - N_R = number of reactions
 - i = node index in the x-direction of the network
 - j = node index in the y-direction of the network
 - k = node index in the z-direction of the network
 - ip = index for the orientation of a single pore
 - p = pressure, Pa
 - p_i = partial pressure, Pa
 - R = gas constant, $\text{J}/(\text{K mol})$
 - r = rate of reaction, $\text{mol}/(\text{m}^2 \text{ s})$
 - r_p = pore radius, m
 - T = temperature, K
 - V = pore volume, m^3
 - w = length coordinate, m
 - x = mole fraction
 - Z = connectivity, compressibility factor
- Greek Letters**
- β = mass-transfer coefficient, m/s

η = dynamic viscosity, Ns/m²

ν = matrix of the stoichiometric coefficients

ρ_c = density of coke, kg/m³

Subscripts

b = bulk phase

Cp = coke precursor

Cg = growing coke

Ct = terminated coke

t = total coke

i, j = component

m, M = micro, macro

net = network

cat = real catalyst

p = pore

P = pellet

Superscripts

D = diffusive

V = viscous

S = surface

Literature Cited

- Arbab, S.; Sahimi, M. Computer simulations of catalyst deactivation—I. Model formulation and validation. *Chem. Eng. Sci.* 1991a, 46 (7), 1739–1747.
- Arbab, S.; Sahimi, M. Computer simulations of catalyst deactivation—II. The effect of morphological, transport and kinetic parameters on the performance of the catalyst. *Chem. Eng. Sci.* 1991b, 46 (7), 1747–1755.
- Avnir, D., Ed. *The Fractal Approach to Heterogeneous Chemistry*; John Wiley: New York, 1989.
- Beeckman, J. W.; Froment, G. F. Catalyst deactivation by site coverage and pore blockage. *Chem. Eng. Sci.* 1980, 35, 805–815.
- Beeckman, J. W.; Froment, G. F.; Pismen, L. Deactivation of porous catalysts by coke formation. *Chem.-Ing.-Tech.* 1978, 50 (12), 960–961.
- Beyne, A. O. E.; Froment G. F. A percolation approach for the modeling of deactivation of zeolite catalysts by coke formation: Diffusional limitations and finite rate of coke growth. *Chem. Eng. Sci.* 1993, 48 (3), 503–511.
- Bunde, A., Havlin, S., Eds. *Fractals in Science*; Springer-Verlag: Heidelberg, 1994.
- Deufhard, P. *Newton techniques for highly nonlinear problems—theory, algorithms, codes*; Academic Press: New York, 1997, to be published.
- Drewry, H. P. G.; Seaton, N. A. Continuum Random Walk Simulations of Diffusion and Reaction in Catalyst Particles. *AIChE J.* 1995, 41, 880–893.
- Duff, I. S. MA28—a set of FORTRAN subroutines for sparse unsymmetric linear equations. Technical Report R. 8730, AERE, 1977.
- Duff, I. S. Direct methods for solving sparse systems of linear equations. *SIAM J. Sci. Comput.* 1982, 5, 605–619.
- Dullien, F. A. L. *Porous Media—Fluid Transport and Pore Structure*; Academic Press: New York, 1992.
- Foster, R. N.; Butt, I. A. A Computational Model for the Structure of Porous Materials Employed in Catalysis. *AIChE J.* 1966, 12, 180–185.
- Gavalas, G. R.; Kim, S. Periodic Capillary Models of Diffusion in Porous Solids. *Chem. Eng. Sci.* 1981, 36, 1111–1122.
- Hollewand, M. P.; Gladden, L. F. Modeling of diffusion and reaction in porous catalysts using a random three-dimensional network model. *Chem. Eng. Sci.* 1992a, 47 (7), 1761–1770.
- Hollewand, M. P.; Gladden, L. F. Representation of porous catalysts using random pore networks. *Chem. Eng. Sci.* 1992b, 47 (9–11), 2757–2762.
- Hoshen, J.; Kopelman, R. Percolation and cluster distribution. I. Cluster multiple labelling technique and critical concentration algorithm. *Phys. Rev. B* 1976, 14, 3438.
- Hoyer, W.; Schmidt, J. W. Newton-type decomposition methods for equations arising in network analysis. *Z. Angew. Math. Mech.* 1984, 64, 397–405.
- Jerauld, G. R.; Hatfield, J. C.; Scriven, L. E.; Davis, H. T. Percolation and conduction on Voronoi and triangular net-
- works: a case study in topological disorder. *J. Phys. C* 1984, 17, 1519–1529.
- Johnson, M. F. L.; Stewart, W. E. Pore structure and gaseous diffusion in solid catalysts. *J. Catal.* 1965, 4, 248–252.
- Keil, F. J. Modelling of Phenomena within Catalyst Particles. *Chem. Eng. Sci.* 1996, 51, 1543–1567.
- Keil, F. J.; Rieckmann, C. Optimization of three-dimensional catalyst pore structures. *Chem. Eng. Sci.* 1994, 49 (24A), 4911–4822.
- Keil, F. J.; Schreiber, D. Reconstruction of Pore Radii from Diffusion Measurements in Porous Materials. *Chem.-Ing.-Tech.* 1994, 66, 201–203 (in German).
- Liu, H.; Zhang, L.; Seaton, N. A. Determination of the connectivity of porous solids from nitrogen sorption measurements—II. Generalization. *Chem. Eng. Sci.* 1992, 47 (17/18), 4393–4404.
- Mason, E. A.; Malinauskas, A. P. *Gas Transport in Porous Media: The Dusty-Gas Model*; Elsevier: Amsterdam, The Netherlands, 1983.
- McGreavy, C.; Andrade, J. S., Jr.; Rajagopalan, K. Consistent Evaluation of Effective Diffusion and Reaction in Pore Networks. *Chem. Eng. Sci.* 1992, 47, 2751.
- Nowak, U.; Weimann, L. A family of Newton codes for systems of highly nonlinear equations—algorithms, implementation, application. Technical Report TR 90-10, Konrad-Zuse-Zentrum für Informationstechnik, Berlin, 1990.
- Petropoulos, J. H.; Petrou, J. K.; Liapis, A. I. Network Model Investigation of Gas Transport in Bidisperse Porous Adsorbents. *Ind. Eng. Chem. Res.* 1991, 30, 1281–1289.
- Portsmouth, R. L.; Gladden, L. F. Determination of pore connectivity by mercury porosimetry. *Chem Eng. Sci.* 1991, 46, 3023–3036.
- Reyes, S.; Jensen, K. Estimation of Effective Transport Coefficients in Porous Solids Based on Percolation Concepts. *Chem. Eng. Sci.* 1985, 40, 1723–1734.
- Sahimi, M. Transport of Macromolecules in Porous Media. *J. Chem. Phys.* 1992, 96, 4718.
- Sahimi, M. *Flow and Transport in Porous Media and Fractured Rock*; VCH: New York, 1995.
- Scharfenberg, R.; Meyerhoff, K.; Hesse, D. Problems in the determination of pore connectivity by digital image processing. *Chem. Eng. Sci.* 1996, 51, 1889–1896.
- Schmidt, J. W.; Hoyer, W.; Haufe, Ch. Consistent approximation in Newton-type decomposition methods. *Numer. Math.* 1985, 47, 413–425.
- Seaton, N. A. Determination of the connectivity of porous solids from nitrogen sorption measurements. *Chem. Eng. Sci.* 1991, 46 (8), 1895–1909.
- Seaton, N. A.; Walton, J. P. R. B.; Qürke, N. A New Analysis Method for the Determination of the Pore Size Distribution of Porous Carbons from Nitrogen Sorption Measurements. *Carbon* 1989, 27, 853–861.
- Sharratt, P. N.; Mann, R. Some observations on the variation of tortuosity with Thiele-modulus and pore size distribution. *Chem. Eng. Sci.* 1987, 42 (7), 1565–1576.
- Taylor, R.; Krishna, R. *Multicomponent Mass Transfer*; John Wiley: New York, 1993.
- Wakao, N.; Smith, J. M. Diffusion in catalyst pellets. *Chem. Eng. Sci.* 1962, 17, 825–834.
- Winterfeld, P. H.; Scriven, L. E.; Davis, H. T. Percolation and conductivity of random two-dimensional composites. *J. Chem. Phys. C* 1981, 14, 2361–2376.
- Zhang, L.; Seaton, N. A. Prediction of the effective diffusivity in pore networks close to a percolation threshold. *AIChE J.* 1992, 38 (11), 1816–1824.
- Zhang, L.; Seaton, N. A. The application of continuum equations to diffusion and reaction in pore networks. *Chem. Eng. Sci.* 1994, 49 (1), 41–50.

Received for review September 25, 1996
Revised manuscript received May 9, 1997

Accepted May 12, 1997⁸

IE9605847

⁸ Abstract published in *Advance ACS Abstracts*, July 1, 1997.